6.1. Introduction

Composite materials by possessing the properties of dielectric, magnetic properties and high insulation that make them indispensable for meeting the advanced technology applications in electronic, electrical, mechanical, and textiles industries [Mishra *et al.* (2014), Sutar *et al.* (2014), Camargo *et al.* (2009), Haertling *et al.* (1999)]. ABO_3 type complex perovskites based ceramics are the important components of electronic devices such as capacitors, resonators and filters. The physical properties of these oxide materials exhibited dielectric and ferromagnetic behaviors **[**Huízar-Félix *et al.* (2012), Lopes *et al.* (2012), Patra *et al.* (2011), Pu *et al.* (2012)].

Complex perovskites having structure $ACu_3Ti_4O_{12}$ (A=Ca, La, Gd, Sm, Dy, Y and Bi) possessing the high dielectric constant which is independent of temperature (100- 600 K) and frequency (10^2-10^6 Hz) **[**Liu *et al.* (2014), Singh *et al.* (2014), Subramanian *et al.* (2000)]. $CaCu_3Ti_4O_{12}$ (CCTO) posses high dielectric constant, showed the numerous potential technological applications in electronic devices. $Bi_{2/3}Cu_3Ti_4O_{12}$ (BCTO) is isostructural with CCTO structure which has been reported in the earlier literature [Yang *et al.* (2015), Liu *et al.* (2004), Jie *et al.* (2004)**]**. It displayed the similar dielectric response in the temperature range of (100 -600 K) and frequency (10^2-10^6 Hz).

Over the last few decades, Bismuth titanate has interested in many applications i;e, microelectronics, electro-optics and dielectrics devices. Bismuth titanate is the lead free ferroelectric material belonging to the Aurivillius family possessing desirable electrical and electro-mechanical properties for electronic devices **[**Ahn *et al.* (2009), Subbarao, E.C (1962)**]**. Ferroelectric and lead based ferroelectric materials are the most widely used in non-volatile ferroelectric random access memories (FRAM) because of their electrical properties

[Jaffe, B. (2012)]. Undoped $Bi_4Ti_3O_{12}$ (BTO) and lanthanum doped $Bi_{2/3}LaTi_3O_{12}$ (BLTO) ceramic have been shown wide interest in ferroelectric materials because of their applications in non-volatile random access memories [Singh *et al.* (2008), Hu *et al.* (2007), Simões *et al.* (2007)]. These materials are based on the existence of two opposite polarization states which can be used to store binary information in a non-volatile electric field [Hardy *et al.* (2004)]. In industry these materials will be satisfy the several requirements, e.g., a low coercive field, a large remnant polarization and a low processing temperature which is compatible with Si-based IC technology [Lettieri *et al.* (2000), Park *et al.* (1999)].

Composite materials are more useful than the individual components or materials. These materials are the mixture of two different or same constituent's material. Their physical and chemical properties were different from their individual materials. Pgautam *et al.* has recently reported the composite having composition 0.5 $Bi_{2/3}Cu_3Ti_4O_{12}$ - 0.5 $Bi_3LaTi_3O_{12}$ which exhibited the high dielectric constant ($\varepsilon' \approx 13.94 \times 10^3$ at 100 Hz) **[**Gautam *et al.* (2017)**]**. Here in, we have synthesized the new composition of 0.9 $Bi_{2/3}Cu_3Ti_4O_{12}$ - 0.1 $Bi_3LaTi_3O_{12}$ (BCLT-91) composite fabricated by semi wet route and reported the effect of electrical, dielectric and magnetic properties of the composite with frequency and temperature.

6.2. Experimental

0.9 $Bi_{2/3}Cu_3Ti_4O_{12}$ - 0.1 $Bi_3LaTi_3O_{12}$ (BCLT-91) composite was prepared by the mixing of individual materials of (BCTO) and (BLTO) obtained by semi-wet route. $Bi_{2/3}Cu_3Ti_4O_{12}$ (BCTO) and $Bi_3LaTi_3O_{12}$ (BLTO) materials synthesized by semi-wet route using bismuth nitrate, $Bi(NO_3)_3.5H_2O$ (99.5%; Merck, India), copper nitrate, $Cu(NO_3)_2.3H_2O$ (99.8%; Merck, India), lanthanum oxide, La_2O_3 (99.0%; Merck, India), and titanium oxide,

TiO_2 (99.9%; Merck, India) in the solid state form , were taken in their stoichiometric ratio. A solution of $Bi(NO_3)_3.5H_2O$ and $Cu(NO_3)_2.3H_2O$ were prepared by using distilled water and mixed together in a beaker. The stoichiometric amount of solid TiO_2 and citric acid, $C_6H_8O_7.H_2O$ (99.5%; Merck, India), were added to the solution. The prepared solution was heated on a hot plate at 70-80 °C with continuous stirring to evaporate excess water. After evaporation the water, resulting dry powder of BCTO was calcined at 800 °C for 6 h in the muffle furnace. The similarly the synthesis method of BLTO was same as BCTO ceramic. Further, take an appropriate amount of calcined powders of BCTO and BLTO were mixed with ethanol and grind for 24 h to make a uniform dispersion of the composite. This obtained composite powder was used to make cylindrical pellets on applying 4-5 tons of pressure using 2-3 drops of 2% poly vinyl alcohol (PVA) as a binder. The pellets were preheated to 500 °C for 2 h to remove the binder and finally sintered at 900 °C for 8 h.

The phase formation of composite was identified by X-ray diffractometer (Rigaku miniflex 600, Japan) with Cu-$K_{\alpha,}$ radiation (λ = 1.54 Å) at scanning rate of 2°/min. The particle size of the composite was examined by a transmission electron microscope (TEM, FEI TECANI G^2 20 TWIN, U.S.A.). For TEM analysis of BCLT-91 composite were prepared in acetone using ultra-sonication. The suspensions of composite powder were deposited on the carbon-coated copper grid and dried for 3 h in hot air oven at 60 °C. The microstructure of the composites was examined by a scanning electron microscope (ZEISS, model EVO-18 research; Germany). The elemental analysis of the sintered pellet of BCLT - 91 was carried by EDX (Oxford instrument; USA) attached with SEM. The surface morphology and roughness of BCLT-91 composite were examined using atomic force microscopy (NTEGRA Prima, Germany). For magnetic measurement, a Quantum Design

MPMS-3, (Magnetic property Measurement System) was used over a temperature range 2–300 K and applied a magnetic field of ± 2 tesla. The function of temperature for field cooled (FC) and zero field cooled (ZFC) magnetization at 100 Oe applied field were carried out using SQUID VSM dc magnetometer. The dielectric and electrical properties of the BCLT-91 composite were measured by LCR meter (PSM 1735, Numetri Q 4thLtd. U.K.) with the function of frequency (10 Hz - 5 MHz) at the temperature (300 - 500 K).

6.3. Results and Discussion

6.3.1. Microstructural studies

Fig.6.1 shows the X-ray diffraction pattern (XRD) of BCLT-91 composite sintered at 900 °C for 8 h.

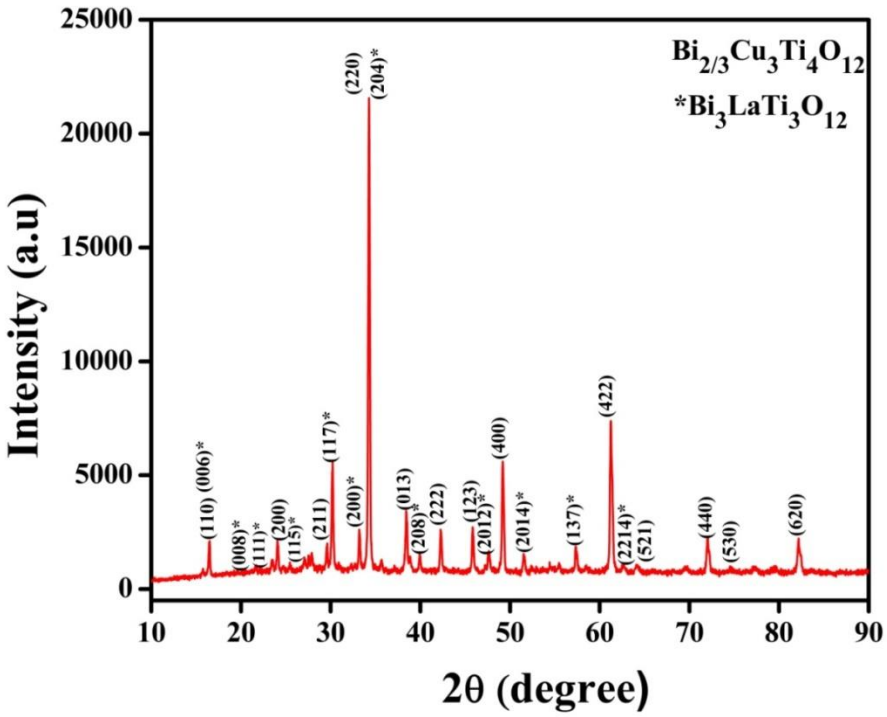

Fig.6.1. XRD patterns of BCLT-91 composite sintered at 900 °C for 8 h.

The X- ray diffraction peaks were indexed JCPDS card and its shows cubic perovskite phase for the BCTO ceramic and tetragonal for BLTO ceramic. The average crystallite size was calculated using line broadening method for BCLT-91 composite. The Cauchy component and Voigt function represent the crystallite size for single-line analysis method. The crystallite size of composite was determined by Scherrer formula [Singh *et al.* (2011)].

$$D = k\lambda/\beta \cos\theta \qquad (6.1)$$

where λ is the wavelength of X-ray, D is the crystallite size, k is a constant taken as 0.89, θ is the Bragg angle of the peaks and β is the full width at half maximum (FWHM) of the peak. The crystallite size of BCLT-91 composite was calculated by using corrected value of β in the above equation. The average crystallite size of the composite was found to be 50.72 nm.

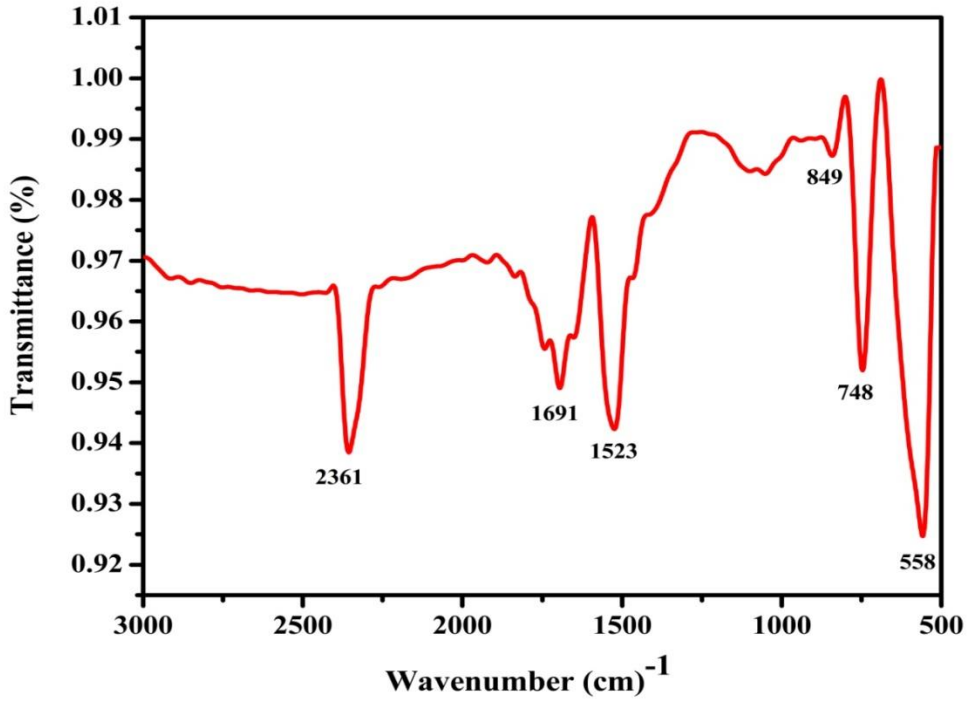

Fig.6.2. FITR spectra for the BCLT-91 composite calcined at 800 °C for 6 h.

FT-IR spectrum of BCLT-91 composite was sintered powder at 900 °C for 8 h shown in Fig.6.2 The peak observed at 1523, 1691 and 2361cm^{-1} explained the OH vibrational mode of the absorbed water molecule **[**Ocwelwang *et al.* (2014)]. The peak observed in low frequency region 558,748 and 849 cm^{-1} were indicating to the Ti-O-Ti, Ti-O band Cu-O stretching vibration, respectively**.** Oxygen–metal bonds were shown in the 400–850 cm^{-1} [Simoes *et al.* (2006), He *et al.* (2006)]. Fig.6.3 exhibited TEM image of BCLT-91 composite sintered at 900 °C for 8 h. Fig.6.3(a&b) shows the crystallite structure of composite in uniform shape and size. However, the particle size was found to be 152 ± 5 nm. Two types of lattice fringes (dark and light fringes) can be seen in Fig.6.3(c).

Table 6.1. Value of d spacing, 2θ and (h k l) correspond to SAED and HR-TEM pattern of BCLT-91 composite.

System	Crystal system	Image used for d values	d-value (nm)	2Θ value (degrees)	(h k l) value	JCPDS card no.
BCTO	Cubic	HR-TEM	0.5244	16.891	1 1 0	
		HR-TEM	0.3708	23.975	2 0 0	80-1343
BCTO	Cubic	SAED	0.1854	49.088	4 0 0	
		SAED	0.1272	74.535	5 3 0	
BLTO	Tetragonal	HR-TEM	0.5511	16.070	0 0 6	
		HR-TEM	0.4117	21.567	0 0 8	50-0278
		HR-TEM	0.3808	23.341	1 1 1	
BLTO	Tetragonal	SAED	0.2573	34.841	2 0 4	

The light fringes define the inter planer spacing (d-spacing) for BLTO ceramic and dark fringes explain to BCTO ceramic, it is observed by h k l value from XRD pattern (JCPDS card no. 50-0278, 80-1343).

Fig.6.3(d) shows selected area diffraction pattern (SAED) of composite. The inter planer spacing was observed cubic phase for BCTO ceramic and tetragonal for BLTO ceramic which is also confirmed by XRD pattern.

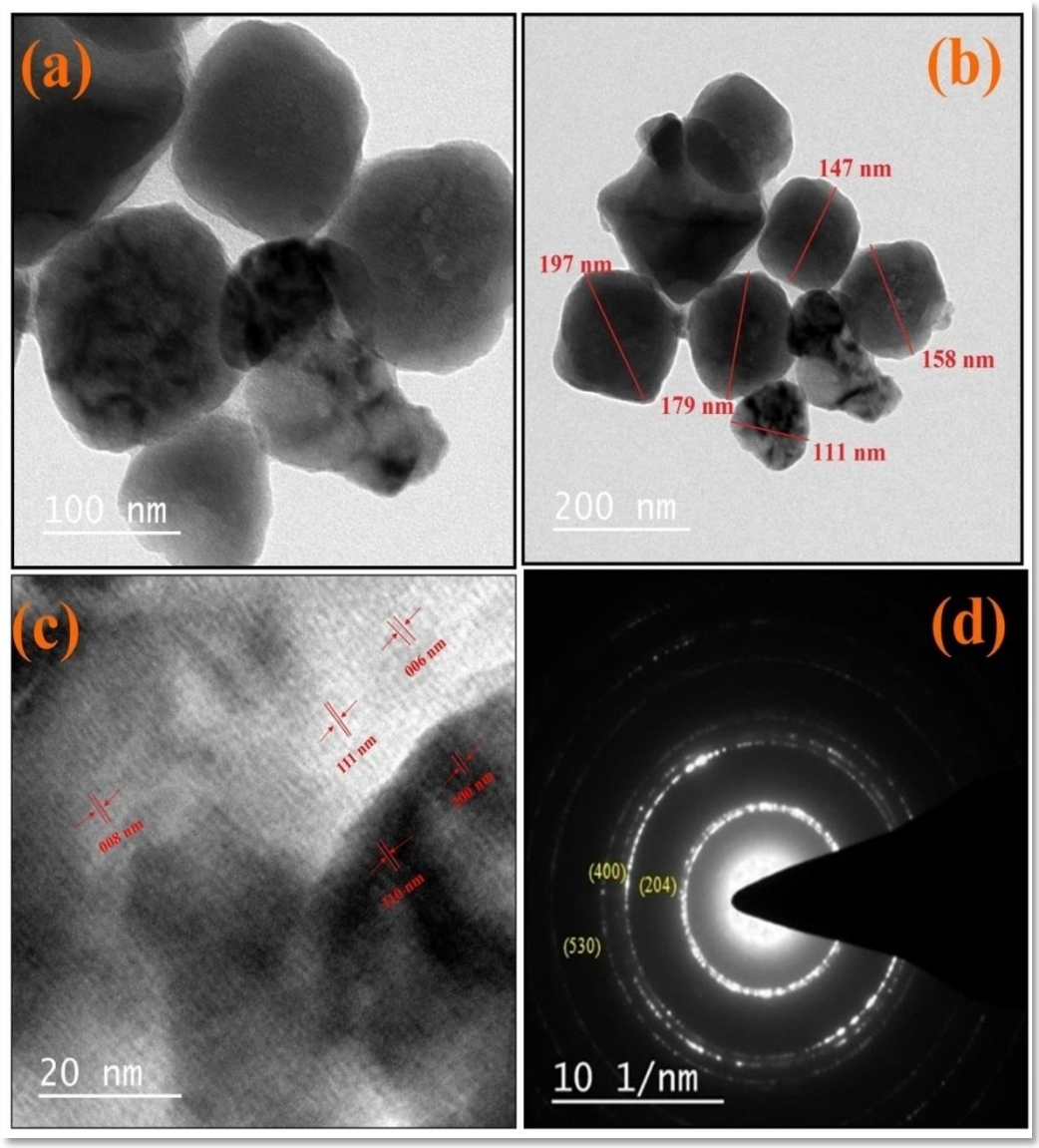

Fig.6.3.(a&b) Bright field TEM image (c) high resolution TEM micrograph (HR-TEM) (d) selected area electron diffraction (SAED) pattern of BCLT-91 composite sintered at 900 °C for 8 h.

The surface morphology obtained by SEM for the composite BCLT-91 was shown in Fig.6.4 It is seen that heterogeneous distribution of grains in the composite. The shape of grains was observed round and plates like **[**Simoes *et al.* (2006)**].** The SEM image was approximately similar to TEM morphology. The average grain size of composite was found to be 0.53 μm.

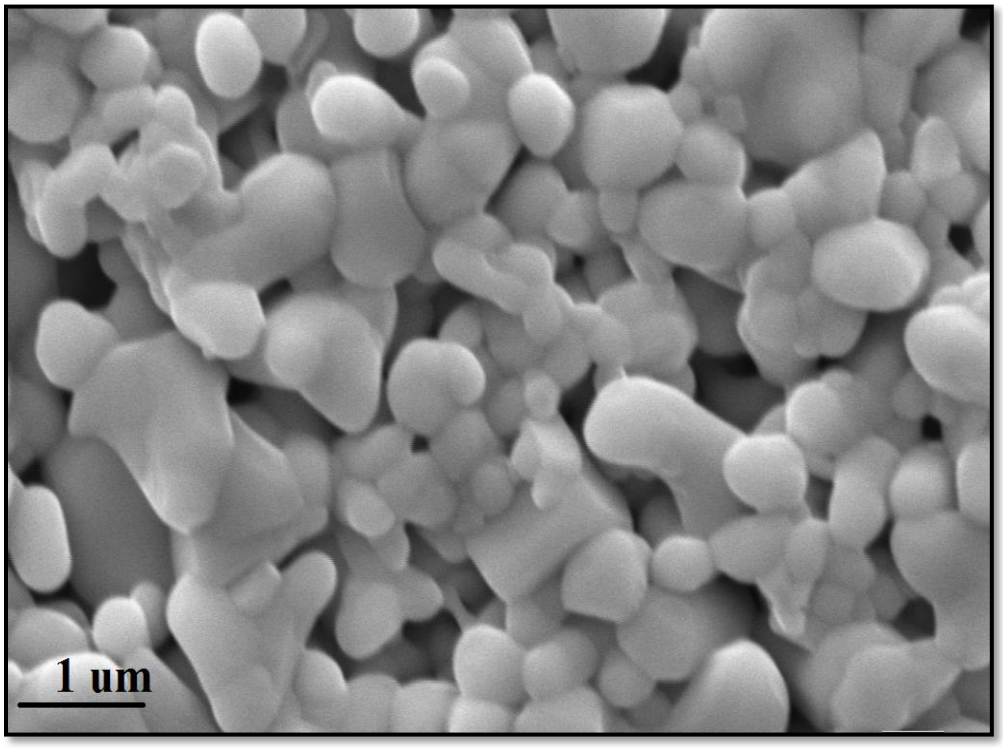

Fig.6.4. SEM image of BCLT-91 composite sintered at 900 °C for 8 h.

Fig.6.5 shows the EDX spectrum of the composite sintered at 900 °C for 8 h. The data of atomic and weight percentage of the elements present in the BCLT-91 composite was obtained from EDX analysis. The atomic percentage of Bi, Cu, La, Ti and O was found to be 4.80, 13.85, 0.18, 20.57 and 60.60, respectively and the weight percentage of composite was

25.97, 22.78, 0.65, 25.50 and 25.10 respectively. It was confirmed that no other impurity was present in the composite from the above mentioned EDX analysis.

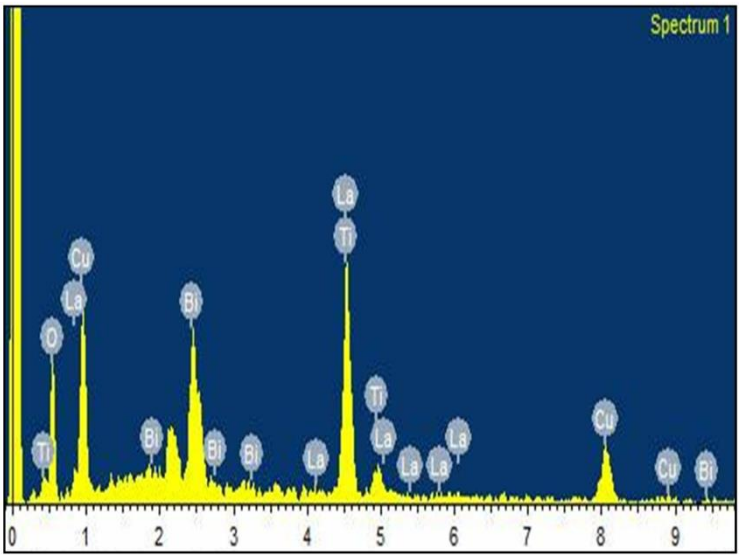

Element	Weight%	Atomic%
Bi M	25.97	4.80
Cu K	22.78	13.85
La L	0.65	0.18
Ti K	25.50	20.57
O K	25.10	60.60
Totals	100.00	

Fig.6.5. EDX spectrum of BCLT-91 composite sintered at 900 °C for 8 h.

AFM morphology of composite sintered at 900 °C for 8 h exhibited in Fig.6.6. The watershed picture of two dimensional images of the composite clearly represented the presence of as grain and grain boundaries (Fig.6.6a). The figure also shows dense structure of

the composite. The three dimensional picture of the composite is shown in Fig. 6.6(b). On the analysis of the figure, the maximum area height peak, maximum area valley depth and root mean square height of the surface were found to be 503.660, 702.375 and143.080 nm, respectively.

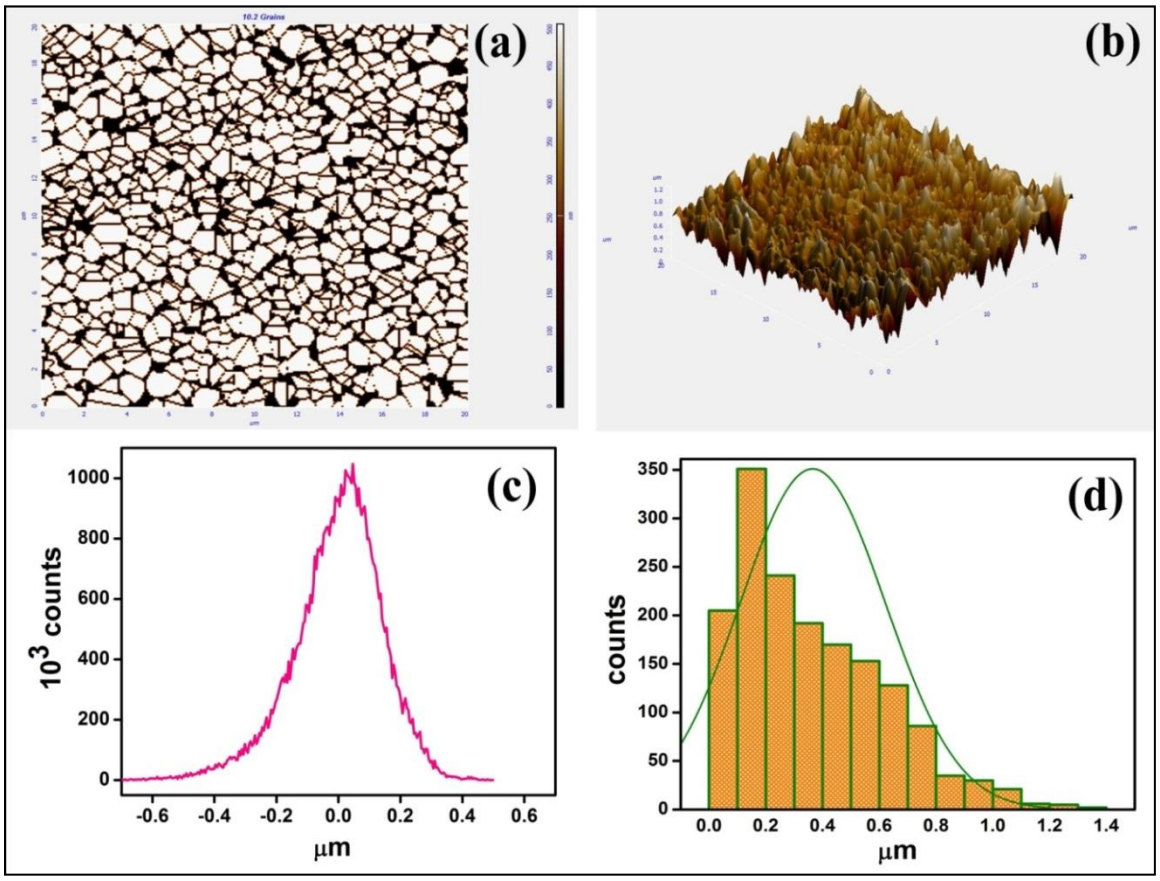

Fig.6.6. AFM images of BCLT-91 composite sintered at 900 °C for 8 h (a) two-dimensional image showing grains and grain boundaries (b) three-dimensional image exhibited high peak distribution (c) histogram of three-dimensional particle roughness and (d) particle size distribution curve.

Fig.6.6(c) shows the histogram of three dimensional picture of the composite from which root mean square roughness and average roughness were calculated and found to be 143.080

nm and 110.381nm, respectively [Khare *et al.* (2016)]. The average grain size was found to be 0.559 μm, out of 811 grains observed by three dimensional images as shown in Fig. 6.6 (d), which was also supported by SEM analysis of the composite.

6.3.2. Magnetic studies

Fig. 6.7(a) shows magnetization curve of field cooled (FC) and zero field cooled (ZFC) for the composite in the temperature range of 2-300 K at an applied magnetic field of 100 Oe.

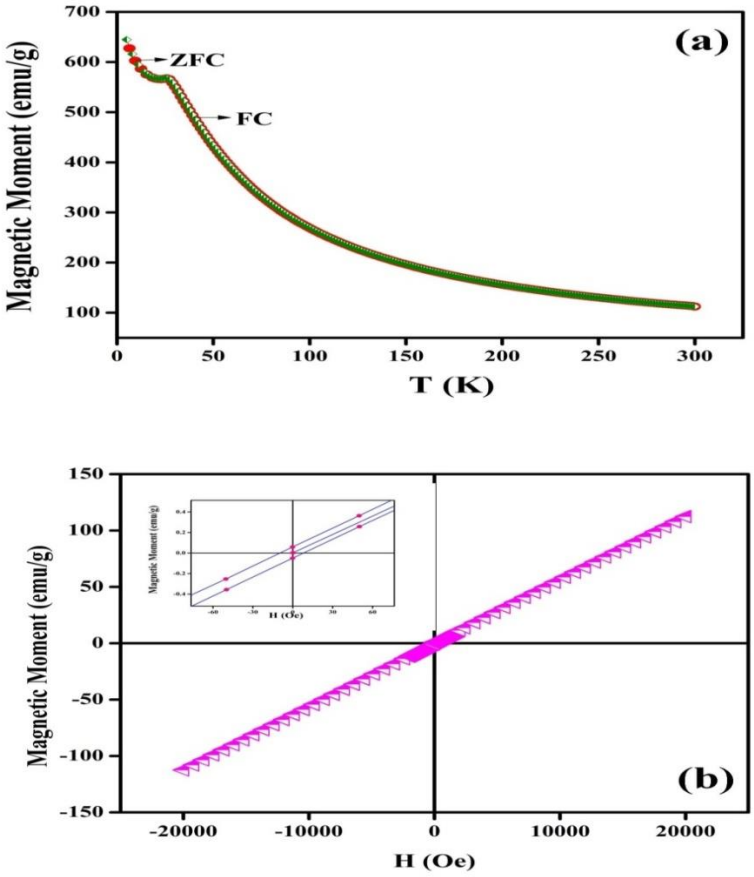

Fig.6.7.(a)Temperature-dependent zero field cooled (ZFC) and field cooled (FC) magnetization measured at H= 100 Oe and (b) magnetization versus applied field at 300 K and inset figure shows coercivity of BCLT-91 composite.

These curves overlap to each other up to a magnetization 566.9 emu/g at 27 K. A broad peak of ZFC and FC was found at 25 K with increasing magnetization, which displayed the magnetic transition from paramagnetic to anti ferromagnetic phase. Fig.6.7(b) shows M-H curve of composite measured at 300 K at an applied field ± 2 T. The curve shows a straight line and unsaturated entity at the temperature. Therefore, the zoom view of hysteresis loop was exhibited in an inset, which is observed that magnetic transition from paramagnetic to weak ferromagnetic behavior [Maaz *et al.* (2010)]. The value coercivity was found to be 24 Oe.

6.3.3. Dielectric studies

Fig.6.8 shows the variation of dielectric constant (ε') and tangent loss (tan δ) with frequency at few selected temperatures. The value of dielectric constant (ε') increases with increasing temperature and decreases with frequency as observed in (Fig.6.8a). The giant value of dielectric constant was found to be 2.3×10^6 at 463 K. The values of dielectric constant of any material depend on the various types of polarizations such as dipolar, electronic, ionic and interfacial polarization [Atyia *et al.* (2007)]. At higher frequency, the dielectric constant responsible for electronic polarization and low frequency exhibited to an interfacial polarization of the materials [Badr *et al.* (2011)]. The increase of dielectric constant with decreasing frequency could be explained on the basis of dipole relaxation phenomenon **[**Thakur *et al.* (2016)]. The variation of tangent loss (tan δ) with frequency at few selected temperatures is observed in Fig.6.8(b).The relaxation peaks appear in tangent loss (tan δ), which shifts towards higher frequencies along with a slight increase in height by increasing temperature. This type of phenomenon mostly shows thermal activated Debye like relaxation. The relaxation behavior of the composite exhibited due to presence of two phases

between grain and grain boundaries with different electrical conductivities are in contact. The similar type of dielectric behavior of the ceramics was reported earlier **[**Thongbai *et al.* (2007), Li *et al.* (2010), Maensiri *et al.* (2007)]**.**

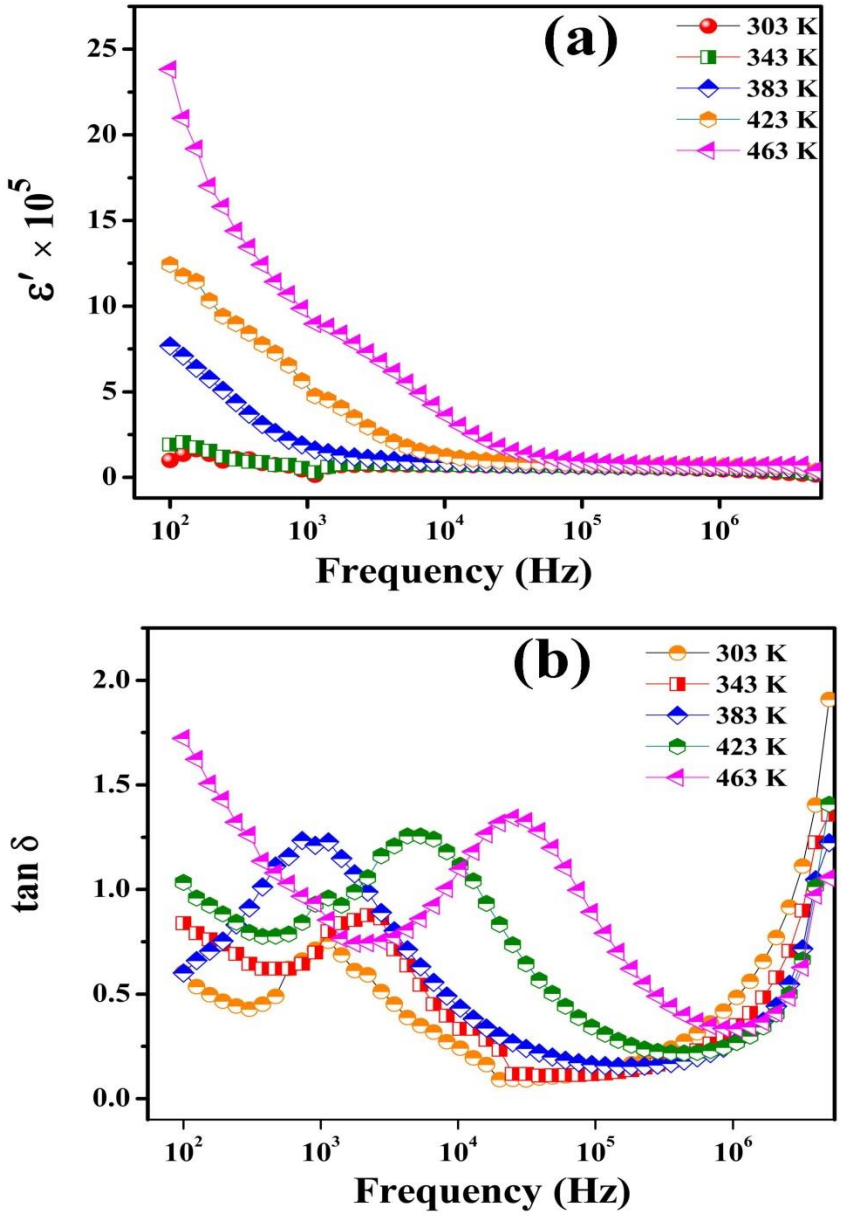

Fig.6.8. Plot of (a) dielectric constant and (b) tan δ as a function of frequency at few selected temperatures for BCLT-91 composite sintered at 900 °C for 8 h.

Fig.6.9 shows the variation of dielectric constant (ε') and tan δ with temperature at few selected frequency. The values of dielectric constant (ε') were found to be 4.0 × 10^6, 14 × 10^5, 6.6 × 10^5 and 1.2 × 10^5at 100 Hz,1 kHz, 10 kHz and 100 kHz at 503 K, respectively (Fig.6.9.a).

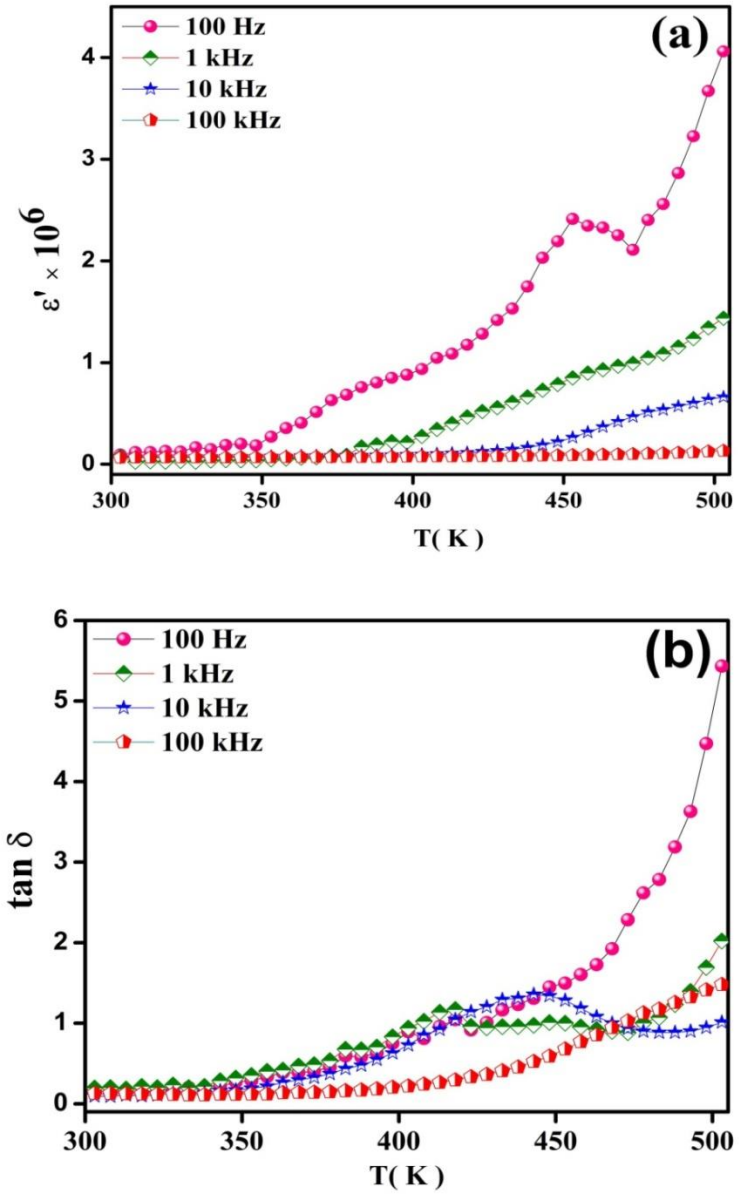

Fig.6.9. Plot of (a) dielectric constant and (b) tan δ as a function of temperature at few selected frequencies for BCLT-91 composite sintered at 900 °C for 8 h.

The value of dielectric constant decreases gradually with increasing frequency at given temperature. Dielectric constant was almost temperature independent at 100 KHz. Fig.6.9(b) shows variation of tan δ with temperature at different frequencies. The value of tan δ that is almost constant for all measured frequencies at 300 K. The relaxation peaks shifted to higher temperature range with increasing frequency. The shifting of relaxation peaks can be also explained by max-well relaxation.

6.4. Conclusion

The 0.9 $Bi_{2/3}Cu_3Ti_4O_{12}$ - 0.1 $Bi_3LaTi_3O_{12}$ composite was synthesized by semi-wet route at low temperature. FT-IR studies confirm the presence of Ti-O, Ti-O-Ti and Cu-O bond in the composite. XRD and TEM studies supported the formation of BCLT-91 composite. Heterogeneous distribution of grains was observed by SEM analysis. The dielectric constant of the BCLT-91 composite was found to be 2.3×10^6 at 463 K and 100Hz. Magnetic measurement of the composite exhibited magnetic transitions from paramagnetic to weak ferromagnetic behavior at 300 K.